Preclinical biomarkers for a cyclin-dependent kinase inhibitor translate to candidate pharmacodynamic biomarkers in phase I patients

Windy Berkofsky-Fessler,[1] Tri Q. Nguyen,[4] Paul Delmar,[4] Juliette Molnos,[4] Charu Kanwal,[1] Wanda DePinto,[2] James Rosinski,[3] Patricia McLoughlin,[4] Steve Ritland,[2] Mark DeMario,[2] Krishna Tobon,[6] John F. Reidhaar-Olson,[1] Ruediger Rueger,[5] and Holly Hilton[1]

[1]RNA Therapeutics, [2]Pharma Development, and [3]In Silico Sciences, Roche, Nutley, New Jersey; [4]Molecular Medicine Laboratories, F. Hoffmann-La Roche Ltd., Basel, Switzerland; [5]Pharma Development, Roche Diagnostics GmbH, Penzberg, Germany; and [6]Department of Pharmacology and Physiology, University of Medicine and Dentistry, New Jersey Medical School, Newark, New Jersey

Abstract

A genomics-based approach to identify pharmacodynamic biomarkers was used for a cyclin-dependent kinase inhibitory drug. R547 is a potent cyclin-dependent kinase inhibitor with a potent antiproliferative effect at pharmacologically relevant doses and is currently in phase I clinical trials. Using preclinical data derived from microarray experiments, we identified pharmacodynamic biomarkers to test in blood samples from patients in clinical trials. These candidate biomarkers were chosen based on several criteria: relevance to the mechanism of action of R547, dose responsiveness in preclinical models, and measurable expression in blood samples. We identified 26 potential biomarkers of R547 action and tested their clinical validity in patient blood samples by quantitative real-time PCR analysis. Based on the results, eight genes (*FLJ44342, CD86, EGR1, MKI67, CCNB1, JUN, HEXIM1,* and *PFAAP5*) were selected as dose-responsive pharmacodynamic biomarkers for phase II clinical trials. [Mol Cancer Ther 2009;8(9):2517–25]

Introduction

Dysregulation of the cell cycle is a hallmark of cancer (1). Cell cycle progression is regulated through the action of cyclin-dependent kinases (CDK) in conjunction with cyclins. CDKs typically remain at a constant concentration, whereas cyclins are present for only a short time in the cell cycle and then are degraded (2, 3). There have been efforts to develop small-molecule pharmacologic inhibitors of CDKs to block tumor cell growth through cell cycle arrest (4–11).

R547 is a potent CDK selective inhibitor (CDK1, CDK2, and CDK4; refs. 12, 13). It has a strong antiproliferative effect at pharmacologically relevant doses in 19 tested cell lines regardless of tissue type, p53, multidrug resistance, or retinoblastoma status. R547-treated cells undergo G_1 and G_2 arrest followed by apoptosis. Preclinical animal studies have shown acceptable toxicity and efficacy in tumor growth inhibition. R547 is currently in clinical phase I studies.

Using preclinical data, we endeavored to identify pharmacodynamic biomarkers with clinical utility. Blood cells are easily accessible and are used in clinical studies as a surrogate tissue to analyze drug activity. Therefore, a focus of this study was the identification of pharmacodynamic markers that would be particularly applicable to circulating WBC in a clinical setting. Here, we describe the identification and assessment of biomarker candidates from preclinical genomics-based studies and their testing in clinical samples. We report the identification of eight genes with potential utility as dose-responsive pharmacodynamic biomarkers for phase II clinical trials.

Materials and Methods

Reagents

R547 [4-amino-2-(1-methanesulfonylpiperidin-4-ylamino) pyrimidin-5-yl]-(2,3-difluoro-6-methoxyphenyl)methanone was synthesized by Discovery Chemistry, Hoffmann-La Roche. Its chemistry, synthesis, and crystallographic structures have been described (12).

Cell Culture

HCT116 ($Rb^+/p53^+$) and DU145 ($Rb^-/p53^-$) cells were maintained as described (13). MTT assays were used to determine dosing: for HCT116 cells, IC_{50} = 0.1 μmol/L R547, IC_{90} = 0.2 μmol/L, and 3× IC_{90} = 0.6 μmol/L; for DU145 cells, IC_{50} = 0.1 μmol/L R547, IC_{90} = 1.7 μmol/L, and 3× IC_{90} = 5.1 μmol/L. HCT116 cells were grown in vehicle (DMSO), IC_{50}, IC_{90}, or 3× IC_{90} dose of R547 for 0, 1, 2, 4, 6, and 24 h. DU145 cells were grown in vehicle (DMSO), IC_{50}, IC_{90}, or 3× IC_{90} dose of R547 for 0, 2, 6, and 24 h. Cells were harvested and lysed in Buffer RLT (Qiagen).

Human peripheral blood mononuclear cells (PBMC) were separated from whole blood of seven healthy donors and cultured in six T75 flasks per donor at 10^7 cells per flask in 10% heat-inactivated fetal bovine serum in RPMI. Cells

Received 2/5/09; revised 6/17/09; accepted 7/10/09; published OnlineFirst 9/15/09.

The costs of publication of this article were defrayed in part by the payment of page charges. This article must therefore be hereby marked *advertisement* in accordance with 18 U.S.C. Section 1734 solely to indicate this fact.

Requests for reprints: Holly Hilton, RNA Therapeutics, Hoffmann-La Roche, Inc., 340 Kingsland Street, Nutley, NJ 07110. Phone: 973-235-2877; Fax: 973-235-2134. E-mail: Holly.Hilton@roche.com

doi:10.1158/1535-7163.MCT-09-0083

from donors 1 to 6 were grown in vehicle, IC_{90} (0.2 μmol/L R547), and 3× IC_{90} (0.6 μmol/L R547) doses of R547 for 2 or 24 h. Donor 7 was used as the untreated 0 h time point. R547 concentrations were based on the HCT116 IC_{90} values. PBMC were scraped and centrifuged for 15 min at 1,500 rpm and the cell pellet was lysed by the addition of 1 mL Buffer RLT.

Microarray Processing

Total RNA was extracted from cells using the Qiagen RNeasy Mini Kit. Total RNA quality was assessed on the Agilent Bioanalyzer 2100.

RNA was converted into cDNA and cRNA according to the manufacturer's recommendation and using the manufacturer's kits (Affymetrix). Total RNA (15 μg) was converted to cDNA with the One-Cycle cDNA Synthesis Kit with the addition of reagents from the Poly-A RNA Control Kit. cRNA was produced with the IVT Labeling Kit. Both cDNA and cRNA were purified with the Sample Cleanup Module. Hybridization Mix contained, in addition to cRNA, reagents from the Hybridization Control Kit and Control Oligo B2.

Hybridization Mix was hybridized to Affymetrix Human Genome U133 Plus 2.0 Arrays. Staining and washing steps were done as suggested by the manufacturer (Affymetrix). Each hybridized Affymetrix GeneChip array was scanned with a GeneChip Scanner 3000 7G (Agilent/Affymetrix). Image analysis was done with the Affymetrix GCOS software.

Microarray Data Analysis

Affymetrix gene expression microarray data (GSE15396 SuperSeries, Gene Expression Omnibus, NIH) was first background-corrected and normalized via the RMA procedure followed by QQ normalization. Quality was assessed through a combination of methods including glyceraldehyde-3-phosphate dehydrogenase ratios, inspection of M/A plots, signal intensity distributions, and RMA residual plots. Quality was very high; only 3 of the 77 HCT116 samples and 7 of the 52 DU145 samples were omitted for quality.

Data for both cell line experiments (HCT116 and DU145) were analyzed in SAS (SAS Institute) via an area under the curve (AUC) method. The cell line experiments were modeled using a linear model including terms for dose, time, and their interaction. AUC was calculated from the linear model as a linear combination of terms using SAS estimate statements. Differences between the AUC values were determined via contrast. From the linear modeling results, "hits" were determined by filtering the *P* values and magnitudes of change for various forms of dose response. In general, the model *P* value was held at a threshold of <0.0001 to control for multiple comparisons; all following contrast *P* values were assessed at a 0.05 threshold.

For the PBMC study, a simpler linear model was used to compare the two doses to the control at the two time points. Hits were selected as probe sets with at least a 2-fold change and $P < 0.05$. The more relaxed *P*-value threshold on this data set reflects the greater variability and lower sample size available for the *ex vivo* samples compared with the cell line data.

Lists were then created of significant hits with specific patterns of dose response in the cell lines or significant changes reflective of dose response in the PBMC (e.g., "responsive at IC_{90} and above" or "responding with dose to a ceiling of the IC_{90}"). These lists formed the basis for further analysis and candidate biomarker selection.

Process of Gene Ranking

Genes were selected for evaluation in clinical samples after consideration of their cellular activity, gene regulation, and biological pathway classification using Ingenuity Pathways Analysis. In addition, the Roche Expression Database of Affymetrix profiling experiments was examined to determine expected expression levels in the blood of cancer patients (Asterand; Proteogenix).

Clinical Trial

Patients were required to be ages ≥18 years with histologically or cytologically confirmed locally advanced solid tumors or chronic lymphocytic leukemia or refractory lymphomas. Patients with solid tumors must have had measurable or evaluable disease by Response Evaluation Criteria in Solid Tumors (14). Other key eligibility criteria include Eastern Cooperative Oncology Group performance status 0 to 2 and adequate bone marrow, hepatic, and renal function, defined as absolute neutrophil count 1,500/μL, platelet count 75,000/μL, hemoglobin 8.0 g/dL, total bilirubin level ≤1.5 mg/dL, aspartate aminotransferase or alanine aminotransferase levels ≤2 times the upper limit of normal or ≤5 times the upper limit of normal if due to liver metastases, and serum creatinine ≤1.5 mg/dL or creatinine clearance ≤60 mL/min. Patients with unstable central nervous system metastases (symptomatic disease requiring steroids or progressive disease by computed tomography/magnetic resonance imaging) were ineligible as were patients with neuropathy grade ≥2, recent myocardial infarction or congestive heart failure, history of cerebrovascular accident, or treatment with chemotherapy, radiotherapy, or immunotherapy within 3 weeks of start of study medication. Clinical characteristics are shown in Table 1.

The clinical study was conducted at four institutions within the United States: University of Colorado Health Sciences Center, University of Texas M.D. Anderson Cancer Center, Cancer Institute of New Jersey, and Carolinas Hematology/Oncology. Patients were required to provide written informed consent before enrollment into the study. Institutional review board approvals were obtained from the participating centers before patient enrollment.

Drug was dosed on days 1 and 8 by 90-min injections (cohorts 1-7) or 180-min injections (cohorts 6A and 7A) every 21 days (Table 2). Two PAXgene tubes (PreAnalytiX, Hombrechtikon) of blood were drawn from each patient on day 1 just before injection of drug (time point 301), 3 h after the completion of injection (time point 302), and on day 2, 24 h after the start of the injection (time point 303). Samples were drawn for the second dose at the same time points 0, 3, and 24 h (304, 305, and 306) on days 8 and 9. There were some missing data points due to patients missing a blood draw or poor sample quality (degraded RNA or low yield).

Table 1. Clinical characteristics

Characteristics	*n*
Age (y)	
Median	54
Mean	54
Min	20
Max	81
Sex, *n*	
M	21
F	24
Diagnosis, *n*	
Bone	1
Breast	6
Colon	6
Kidney	1
Liver	2
Lung	8
Ovary	3
Pancreas	2
Pelvis	1
Prostate	1
Rectum	3
Skin	1
Urinary bladder	1
Other	9
Stage, *n*	
Locoregional	21
Metastatic	24

NOTE: Other: abdomen, adenoid, appendix, left nasal, ocular, right hard palate, scalp, and thymus.

Quantitative Real-time PCR

RNA extraction was done from the PAXgene blood on a BioRobot MDx following the manufacturer's protocol (Qiagen), with omission of the 80°C heating step. RNA was quantified with the Quant-IT RiboGreen kit (Molecular Probes, Invitrogen) at 50-fold dilution against standard curves of *Escherichia coli* ribosomal RNA (Roche Diagnostics).

cDNA synthesis was done with the SuperScript II First-Strand Synthesis SuperMix for quantitative real-time PCR (qRT-PCR; Invitrogen) on 400 ng total RNA following the manufacturer's protocol but with omission of the RNase H digest. For each reverse transcription reaction, Universal Human Reference total RNA (Stratagene) was run as a positive and negative control (nonenzyme control) on the same plate. Controls were assayed by qRT-PCR.

Predesigned gene expression assays were obtained from Applied Biosystems. Where possible, exon-spanning assays were selected to ensure cDNA specificity. In addition, assays were selected to lie either within the Affymetrix probe sequence of interest or as 3′ as possible within the coding sequence of the reference mRNAs of interest. One assay was custom designed. All gene expression assays were done on an ABI PRISM 7900HT Sequence Detection System (Applied Biosystems) with the recommended standard settings. All assays were prepared with the TaqMan Universal PCR Master Mix (Applied Biosystems) following the manufacturer's recommendations. All runs included a standard curve dilution of cDNA, a nonenzyme control, a nontemplate control, and a calibrator sample. Standard curve cDNA was synthesized from Universal Human Reference total RNA (Stratagene) and the calibrator sample from a pool of total blood RNA from healthy donors. cDNA samples were diluted 10-fold in molecular-grade water, and 2 μL were added to 18 μL predistributed assay Master Mix. This corresponds to cDNA from 4 ng total RNA. All samples on a plate were assayed with one assay for a gene of interest and the endogenous control gene assay, GUSB (β-glucuronidase, TaqMan Gene Expression Assays; Applied Biosystems). Each measurement was done in triplicate.

Statistical Analysis of qRT-PCR Data

ΔCt values were used for statistical analysis. The nonparametric Jonckheere-Tepstra back (J-T test) trend test was used to test for a consistently increasing or decreasing relationship between dose and gene expression level (monotonic dose-response trend with expression). Additionally, AUC- and C_{max}-based tests were done, testing for diffe-rences across the doses (data not shown).

For graphical representation for data analysis, both -ΔΔCt values and fold changes were used. Fold changes are calculated from ΔΔCt with the following formula: $2^{-\Delta\Delta Ct}$. ΔΔCt is defined as the normalized value of ΔCt using time point 301 or 304 as a reference.

Results

To identify candidate biomarkers, we chose two proliferating cancer cell lines (the HCT116 colon cancer cell line and the DU145 prostate cancer cell line) and nonproliferating PBMC as a surrogate for normal tissue. We conducted a series of expression profiling experiments using Affymetrix GeneChip arrays (for detailed diagram, see ref. 15), designed to determine the dose responsiveness (vehicle, IC_{50}, IC_{90}, and 3× IC_{90}) of these cells to the CDK inhibitor R547 over varying time points (0, 1, 2, 4, 6, and 24 h). Numbers of genes found to be differentially expressed in a dose-responsive manner in the different comparisons are shown in Fig. 1. These genes were narrowed to 88 by several criteria. First, all genes dysregulated on treatment with R547 common to the PBMC and either or both cell lines were included

Table 2. Patient cohort assignment

Cohort	Dose (mg/m^2)	Administration duration (min)	No. patients
1	8.6	90	4
2	17.2	90	5
3	34.4	90	4
4	69	90	3
5	105	90	4
6	155	90	8
6A	155	180	6
7	195	90	3
7A	195	180	8

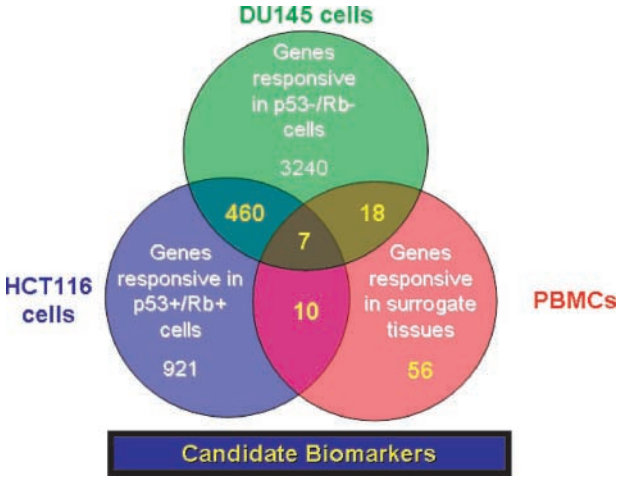

Figure 1. Diagram showing method of microarray analysis to isolate possible biomarkers. Each experimental model is represented by a different colored circle: *blue circle,* HCT116 cell line; *green circle,* DU145 cell line; *red circle,* PBMC. All genes that were differentially expressed in either HCT116 or DU145 cell line and PBMC plus selected genes differentially expressed in both HCT116 and DU145 or in the PBMC comprised our candidate biomarkers (*yellow*).

based on the hypothesis that PBMC, being nondividing primary human cells, are most similar to patient blood samples. Next, we selected genes with the highest fold changes from the genes significantly ($P \leq 0.05$) dysregulated on treatment in the PBMC alone. Top differentially expressed genes (both up-regulated and down-regulated) in the overlap of the two cell lines were also included because these genes may better represent cancer cells.

We ranked the 88 genes based on personal expertise (15) and the following four criteria: (*a*) The gene was mechanistically related to the action of the compound based on literature and pathway analysis. (*b*) The gene was expected to be detectable in blood based on its expression level in the PBMC data set and in the Roche Expression Database containing donor whole-blood samples collected in RNA PAXgene tubes. (*c*) The expression levels of the gene showed a dose response. (*d*) Avoid genes with expression that changes in response to many oncology compounds.

The top 26 genes from this set were chosen for analysis in the human phase I patient samples (Table 3). The assays for all genes, except *CCL7*, showed measurable amplification in preliminary blood samples and were subsequently run on the clinical blood samples. A variety of measures were used to assess the robustness and quality of the measurements and technologies, including median Ct level, the range of technical triplicates, the directionality of the expression change as measured by gene expression microarray and qRT-PCR, and the level of significance of any changes in expression of the endogenous control gene compared with that of the target gene.

After reviewing the qRT-PCR fold changes (Tables 3 and 4) and robustness of PCR assays, the genes were ranked as candidate biomarkers. The top four genes were *FLJ44342*, *CD86*, *EGR1*, and *MK167* (Fig. 2, *top*). The second tier genes *CCNB1*, *JUN*, *HEXIM1*, and *PFAAP5* are shown in Fig. 2 (*bottom*). These genes all showed a statistically significant dose response to R547. Nine genes showed a borderline or incomplete pattern of significance in the dose response (*CALM2*, *CES1*, *CHN2*, *KITLG*, *KRAS*, *NME1*, *PRDM2*, *SAP30*, and *STAT3*). Eight genes showed no correlation between treatment and expression level (*BCCIP*, *BUB3*, *CDC14B*, *MAF*, *MAP3K5*, *PAIP1*, *PHDLA1*, and *WEE1*) despite the response in the preclinical studies.

Table 3 details the fold changes for each gene in the three preclinical microarray studies as well as the qRT-PCR results from the clinical blood samples. Table 4 shows the results of statistical testing for genes showing a significant dose response (boldfaced genes were significant).

The qRT-PCR results (Table 3) for cDNA *FLJ44342* validated the microarray results for PBMC. CD86 (B-lymphocyte activation antigen b7-2) had a highly significant down-regulation in the higher dose groups at the 3 h time point, which returned to baseline after 24 h; this pattern was repeated in the second dose. *EGR1* (early growth response 1) was up at the 3 h time point and returned to baseline by the 24 h time point as measured by qRT-PCR, although there were mixed results with microarray. *MKI67* (proliferation-related Ki-67 antigen) first increased and then decreased below baseline by qRT-PCR and showed a decrease in all microarray experiments. *CCNB1* (cyclin B1) was down-regulated in a dose-dependent fashion at both the 3 h time point and the 24 h time point by qRT-PCR and by microarray (data not shown). A decrease in JUN (V-*JUN* avian sarcoma virus 17 oncogene homologue) was seen in most conditions by both qRT-PCR and Affymetrix. *HEXIM1* (hexamethylene bisacetamide-inducible protein 1) was up by qRT-PCR in these studies. *PFAAP5* (N4BP2L2, NEDD4 binding protein 2-like 2) was down at the 3 h time point by qRT-PCR, although the results were mixed by microarray.

Discussion

Preclinical genomics models of the CDK inhibitor R547 have proven to be predictive of drug-responsive genes in oncology patients. A multidisciplinary process of gene selection from several preclinical Affymetrix GeneChip experiments identified a panel of potential pharmacodynamic biomarkers. Eight of these genes changed clinically in a dose-responsive fashion, indicating that the drug is reaching its target. More detailed exploration of these top eight genes revealed seven with known links to cancer and one that was unknown (*FLJ44342*).

cDNA *FLJ44342* is interrogated by the Affymetrix probe set 226419_s_at. At the time of gene selection for this study, this probe set was annotated as belonging to a 5′ exon of *SFRS1*. When selecting qRT-PCR assays for each gene, we discovered that it was no longer annotated as such. We therefore designed primers and probes to the same region as the Affymetrix probe set. The transcript for this gene, Q6ZTQ9_Human, is an Ensembl Known Protein Coding region, located between the genes for VEZF1 and SFRS1 on chromosome 17q23.2 (16). The protein is not a member of

Table 3. Median fold changes for genes selected preclinically for RT-PCR follow-up in patient samples from the clinical trial

Probe set ID	Gene symbol	Gene title	Entrez gene ID	Affymetrix median fold changes (preclinical; compared with 0 h)						RT-PCR median fold changes for all patients in cohort 6A (clinical; compared with pretreatment)			
				HCT116		DU145		PBMC		Cycle 1		Cycle 2	
				2 h	24 h	2 h	24 h	2 h	24 h	302 (3 h)	303 (24 h)	305 (3 h)	306 (24 h)
227322_s_at	BCCIP	BRCA2 and CDKN1A interacting protein	56647	−1.20	−1.22	1.14	−1.57	−1.21	1.16	1.44	1.14	1.55	1.03
201457_x_at	BUB3	BUB3 budding uninhibited by benzimidazoles 3 homologue (yeast)	9184	−1.12	−2.22	−1.01	−3.94	−1.51	−1.08	−1.03	−1.13	1.22	−1.16
207243_s_at	CALM2	Calmodulin 2	805	−1.26	−1.45	1.00	−6.54	−1.03	−1.11	−1.52	1.37	−1.04	1.37
208075_s_at	CCL7	Chemokine (C-C motif) ligand 7	6354	1.14	1.07	1.01	1.47	1.70	11.07	NA	NA	NA	NA
214710_s_at	**CCNB1**	**Cyclin B1**	**891**	**−1.35**	**−7.16**	**−1.14**	**−24.33**	**−1.28**	**−1.10**	**−1.48**	**−1.18**	**−1.22**	**−1.12**
210895_s_at	**CD86**	**CD86 molecule**	**942**	**1.06**	**1.13**	**1.09**	**1.06**	**−1.53**	**−1.89**	**−4.05**	**1.16**	**−3.57**	**1.16**
221555_x_at	CDC14B	CDC14 cell division cycle 14 homologue B	8555	−1.07	−1.12	−1.53	−8.02	−1.20	−1.60	1.12	1.13	1.33	1.02
209616_s_at	CES1	Carboxylesterase 1	1066	−1.05	1.13	−1.06	1.33	1.94	4.90	1.05	1.93	−1.45	2.06
213385_at	CHN2	Chimerin (chimaerin) 2	1124	−1.01	1.08	−1.10	−1.16	−2.18	−2.14	−1.18	1.13	−1.33	1.05
227404_s_at	**EGR1**	**Early growth response 1**	**1958**	**−1.14**	**−1.05**	**−10.50**	**12.82**	**1.03**	**−1.53**	**1.70**	**1.13**	**1.53**	**1.25**
226419_s_at	**FLJ44342**	**Hypothetical LOC645460**	**645460**	**1.56**	**−1.12**	**−2.00**	**−1.55**	**3.69**	**2.37**	**3.49**	**−1.34**	**3.81**	**1.07**
202814_s_at	**HEXIM1**	**Hexamethylene bisacetamide inducible 1**	**10614**	**−1.86**	**−1.88**	**−1.96**	**−4.10**	**−3.83**	**−3.45**	**1.31**	**1.21**	**1.96**	**1.31**
201464_x_at	**JUN**	**Jun oncogene**	**3725**	**−1.17**	**1.88**	**−5.42**	**6.94**	**−1.44**	**−1.05**	**−1.66**	**−1.00**	**−1.70**	**1.11**
226534_at	KITLG	KIT ligand	4254	−1.07	−1.29	−1.11	−6.97	8.71	2.33	1.56	1.41	2.43	1.38
214352_s_at	KRAS	v-Ki-ras2 Kirsten rat sarcoma viral oncogene homologue	3845	−1.20	−1.39	−1.38	−8.62	−1.05	1.38	−1.10	1.51	1.16	1.36
209348_s_at	MAF	v-maf musculoaponeurotic fibrosarcoma oncogene homologue	4094	1.03	1.04	−1.02	1.27	−1.99	−2.18	−1.30	−1.17	−1.23	−1.07
203836_s_at	MAP3K5	Mitogen-activated protein kinase kinase kinase 5	4217	1.17	−1.41	1.02	−3.55	1.01	−1.18	1.29	1.25	1.74	1.48
212021_s_at	**MKI67**	**Antigen identified by monoclonal antibody Ki-67**	**4288**	**−1.27**	**−6.70**	**−1.03**	**−4.21**	**−1.02**	**−1.12**	**1.30**	**−1.36**	**1.77**	**−1.12**
214748_at	**PFAAP5**	**NEDD4 binding protein 2-like 2**	**10443**	**−1.10**	**1.20**	**−1.02**	**1.17**	**2.15**	**2.48**	**−2.35**	**1.43**	**−1.65**	**1.26**
201577_at	NME1	Nonmetastatic cells 1, protein (NM23A)	4830	−1.09	1.12	1.10	1.26	2.19	2.21	−1.43	1.44	−1.52	1.32
209064_x_at	PAIP1	Poly(A) binding protein interacting protein 1	10605	−1.47	−1.54	−1.08	−19.18	−2.78	−2.01	1.06	−1.02	1.14	1.17
225842_at	PHLDA1	Pleckstrin homology-like domain, family A, member 1	22822	−1.33	1.07	−1.99	−6.16	2.98	2.90	−1.13	−1.11	−1.27	−1.07
205277_at	PRDM2	PR domain containing 2, with ZNF domain	7799	1.29	1.41	−1.05	1.28	2.43	2.19	1.28	−1.23	1.64	−1.17
204900_x_at	SAP30	Sin3A-associated protein, 30 kDa	8819	−1.53	−3.72	1.10	−5.95	−2.49	−2.32	1.63	1.22	1.35	1.34
208991_at	STAT3	Signal transducer and activator of transcription 3	6774	−1.11	1.46	1.04	1.36	−1.29	−1.01	−1.37	1.34	1.10	1.75
212533_at	WEE1	WEE1 homologue (*Schizosaccharomyces pombe*)	7465	−3.77	−4.77	−2.75	−10.88	−1.39	−1.39	−1.26	−1.15	1.30	1.12

NOTE: Boldface indicates selection as top biomarker. Fold changes are up-regulation, except where denoted by (−) to signify down-regulation. See Materials and Methods for discussion of time points assayed.

any known family but does contain a low complexity region and a signal peptide cleavage site.

CD86 is expressed on the surface of antigen-presenting cells (17). It was found to be expressed at higher levels in thyroid carcinoma than in normal thyroid and there was a trend for higher tumor recurrence in CD86-expressing tissues (18). Given these findings, a cancer therapeutic agent should act to lower the levels of this gene in tissues as seen in this study both preclinically and in phase I patients.

The literature on EGR1 is mixed. Microvascular endothelial cell growth, neovascularization, tumor angiogenesis, and tumor growth are all critically dependent on EGR1 (19). Apoptosis requires intact EGR1 as well as p53 (20), but EGR1 confers resistance to apoptosis signals through inhibition of Fas expression leading to insensitivity to FasL (21). $EGR1^{-/-}$ mice have decreased progression of prostate cancer (22). However, studies suggest that it is a tumor suppressor gene (23). EGR1-dependent expression of TGFB1 inhibited cancer growth in cell lines (24) and some human tumor lines have little or no EGR1 compared with normals (25). The qRT-PCR and Affymetrix results from our studies fit with the expectation that an anticancer agent would increase tumor suppressor genes.

MK167 is a marker of proliferating cells (26). Its expression might be necessary for proliferation. Frameshift mutations have been found in gastric carcinoma (27) and its up-regulation has been associated with renal cell carcinoma (28). Our results showing a decrease in the expression of this gene is suggestive of slowing cell proliferation.

Up-regulation of CCNB1 is associated with numerous forms of cancer including lung cancer (29) and breast cancer (30). This gene product forms a complex with p34 (cdc2) creating maturation promoting factor driving the G_2-M transition (31). CDC2, also known as CDK1, is a direct target of R547 (13). Interestingly, although there was no change in cdc2 at the mRNA level, there was a decrease in transcription of CCNB1 both in the preclinical Affymetrix studies and in the phase I qRT-PCR analyses. It has been shown that decreased CCNB1 levels via small interfering RNA led to delay in formation of the metaphase plate and of mitosis progression but not cell cycle arrest due to the loss of the spindle checkpoint (through the loss of CCNB1; refs. 32, 33).

Jun is a known oncogene. Mutant Jun is associated with breast cancer in humans (34). Chemically induced hepatocellular carcinoma produces fewer tumors of smaller size on inactivation of Jun (35). Our studies showed a decrease in this transcript in most conditions.

HEXIM1 competes with C2TA for binding to CCNT1. When C2TA binds CCNT1, it forms positive transcription elongation factor b (P-TEFb) complex that turns on

Table 4. *P* values resulting from statistical testing of qRT-PCR results

Gene	Administration 1				Administration 2			
	Time point 302 (3 h)		Time point 303 (24 h)		Time point 305 (3 h)		Time point 306 (24 h)	
	J-T test for trend, *P*	$\log_2$ (AUC) *P*, line of best fit	J-T test for trend, *P*	$\log_2$ (AUC) *P*, line of best fit	J-T test for trend, *P*	$\log_2$ (AUC) *P*, line of best fit	J-T test for trend, *P*	$\log_2$ (AUC) *P*, line of best fit
BCCIP	0.18	0.15	0.28	0.99	0.42	0.45	0.64	0.43
BUB3	0.35	0.91	0.16	0.19	0.46	0.81	**0.038**	**0.014**
CALM2	0.49	0.3	0.2	0.11	**0.047**	0.053	0.3	0.98
CCNB1	**0.024**	**0.021**	**0.0018**	**0.0018**	0.25	0.12	0.43	**0.027**
CD86	**7.00E-06**	**6.00E-07**	0.40	0.29	**1.10E-05**	**4.50E-06**	0.13	0.98
CDC14B	**0.003**	**0.0019**	0.08	**0.016**	0.09	0.13	0.087	0.48
CES1	0.83	0.25	**0.0002**	**0.0018**	0.2	0.3	**0.0049**	**0.011**
CHN2	**0.016**	**0.023**	0.61	0.14	**0.022**	**0.049**	0.6	0.66
EGR1	**0.0022**	**0.0019**	0.68	0.75	**7.70E-05**	**4.00E-05**	**0.0095**	**0.003**
FLJ44342	**1.90E-07**	**1.50E-09**	**0.04**	0.17	**2.50E-06**	**1.60E-07**	0.71	0.68
HEXIM1	**0.00012**	**0.00053**	0.34	0.16	**3.60E-05**	**2.40E-06**	0.12	**0.0047**
JUN	**0.0059**	**0.0062**	0.079	0.62	**0.05**	**0.0037**	0.44	0.6
KITLG	**0.027**	**0.00098**	0.67	0.11	0.35	0.14	0.95	0.38
KRAS	**0.00037**	**0.0059**	0.13	0.14	0.18	**0.045**	0.39	0.6
MAF	**0.021**	0.13	0.083	0.18	0.1	**0.015**	0.38	0.19
MAP3K5	**0.0033**	**0.00051**	0.22	0.074	0.081	**0.0084**	**0.03**	**0.025**
MKI67	**2.60E-05**	**4.10E-06**	0.08	0.06	**0.001**	**0.00049**	0.083	0.22
NME1	**0.0074**	**0.034**	**1.70E-05**	**1.80E-06**	**0.049**	0.088	**0.0012**	**0.00056**
PAIP1	0.58	0.27	1	0.54	0.64	0.61	0.087	**0.0098**
PFAAP5	**0.039**	**0.016**	0.15	0.18	0.092	**0.015**	0.58	0.34
PHDLA1	**0.006**	**0.00041**	0.065	0.054	0.14	0.58	0.62	0.8
PRDM2	0.76	0.97	0.22	0.89	0.37	0.42	**0.011**	0.2
SAP30	**0.048**	0.32	0.77	0.88	**0.043**	0.15	0.45	0.36
STAT3	0.39	0.12	0.24	0.065	0.15	0.11	**0.0028**	**0.00025**
WEE1	0.71	0.8	**0.022**	**0.03**	**0.024**	0.25	0.3	**0.049**

NOTE: Shading: top eight genes; Boldface indicates $P \leq 0.05$. J-T, Jonckheere-Tepstra.

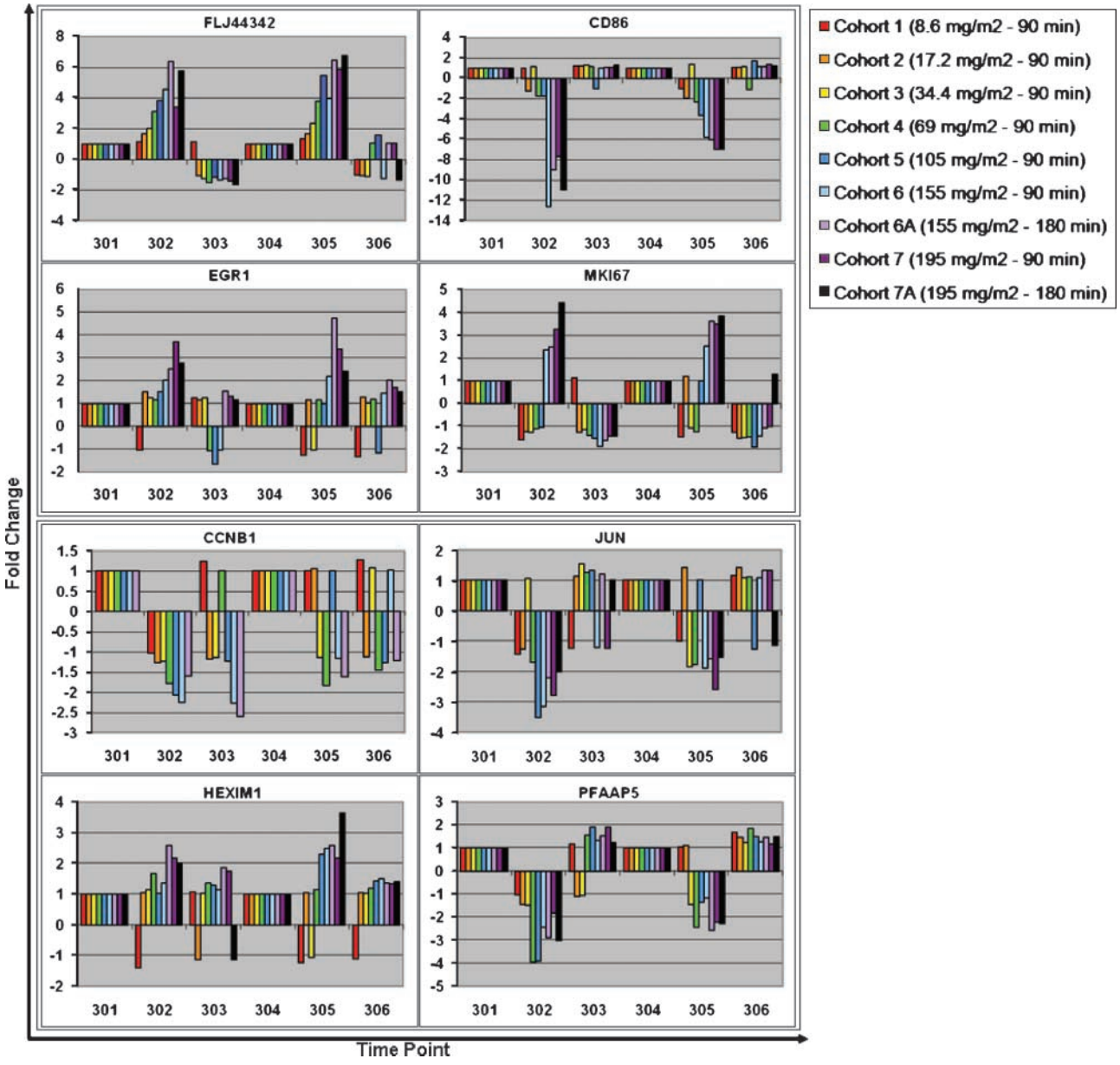

Figure 2. Mean fold change within each cohort by time point for the top four biomarkers (*top*) and the second tier (*bottom*). *X axis,* different time points (see Materials and Methods for further discussion) at which clinical samples were taken; *Y axis,* fold change (calculated by $-\Delta\Delta Ct$) of each sample compared with its baseline time point.

transcription of MHCII genes. If HEXIM1 were up, it would block MHCII gene transcription by sequestration of CCNT1 (36). CDK9 and CCNT1 are binding partners with approximately 80% of CDK9 complexed with CCNT1 (37). Each CDK9/CCNT1 complex is an active P-TEFb molecule that can phosphorylate the COOH-terminal domain of the largest subunit of RNA polymerase II, facilitating the transition from abortive elongation to productive elongation (38). About half of P-TEFb exists in an inactive complex with 7SK (which inhibits CDK9 kinase activity) and HEXIM1 protein. The other half is competitively associated with BRD4 and is active (39). Given that HEXIM1 was up by qRT-PCR, we can hypothesize that more P-TEFb was inactive, thus decreasing the levels of overall transcription.

The function of the PFAAP5 protein is not understood, although it contains a polynucleotide kinase domain [ref. 40; CNPase domain (41)] and has been included in a 19-gene pancreatic cancer–specific expression profile (42). It is upregulated by TP73 (43). TP73 is downstream of ATM/cABL, blocks G_1-S transition, and induces apoptosis (44). Also downstream of ATM/cABL is Jun (45), which has the alternate effect on the G_1-S transition.

The genes selected for qRT-PCR follow-up covered several different interesting patterns and were not always the most obvious choices from either a single statistical or biological perspective. For example, CD86 was chosen based on high blood expression level and adequate fold change in PBMC with limited biological evidence for its selection. However, in patients, this gene had a near ideal result, that is, the highest fold change and most significant response to R547 in patients. This gene was the only one of the top eight to come exclusively from the PBMC data, whereas another gene with more biological rationale for its selection, MAF, had a similar preclinical pattern but did not show a response in patients. Three of the most responsive genes in the clinical samples (FLJ44342, HEXIM1, and PFAAP5) were top hits in all three of the preclinical experiments, whereas the four remaining top hits were only derived from the two cell line experiments. This suggests that use of a wide variety of preclinical models is most effective for the identification of predictors of response in patient blood samples. Additionally, as shown for FLJ44342, even if a probe set interrogates an unnamed gene, it can still be biologically responsive and therefore, of interest.

In conclusion, our rate of success was ~8 genes confirmed of 26 tested suggesting that, in the early phases of development, inclusion of ≥20 genes (within hospital guidelines) may be necessary to detect a pharmacodynamic signal and be most effective for narrowing a list down to a manageable number of pharmacodynamic biomarkers. In addition, these data also suggest that the CDK inhibitor R547 affects physiologic pathways in patients well enough to predict these expression changes in whole-blood samples. Finally, the data suggest that these eight genes could be used to further understand a potentially variable response to our drug among patients in phase II (efficacy) clinical trails.

Disclosure of Potential Conflicts of Interest

All authors are current or former employees of Hoffmann-La Roche.

Acknowledgments

We thank Hongjin Bian and Lyubomir Vassilev for critical discussions and the Cooperative Human Tissue Network for the tissues queried in the Roche Expression Database.

References

1. Sherr CJ. Cancer cell cycles. Science 1996;274:1672–7.

2. Harper JW, Adams PD. Cyclin-dependent kinases. Chem Rev 2001; 101:2511–26.

3. Pines J. Cyclins: wheels within wheels. Cell Growth Differ 1991;2: 305–10.

4. Senderowicz AM, Sausville EA. Preclinical and clinical development of cyclin-dependent kinase modulators. J Natl Cancer Inst 2000;92:376–87.

5. Knockaert M, Greengard P, Meijer L. Pharmacological inhibitors of cyclin-dependent kinases. Trends Pharmacol Sci 2002;23:417–25.

6. Benson C, Kaye S, Workman P, Garrett M, Walton M, de Bono J. Clinical anticancer drug development: targeting the cyclin-dependent kinases. Br J Cancer 2005;92:7–12.

7. Emanuel S, Rugg CA, Gruninger RH, et al. The *in vitro* and *in vivo* effects of JNJ-7706621: a dual inhibitor of cyclin-dependent kinases and aurora kinases. Cancer Res 2005;65:9038–46.

8. McClue SJ, Blake D, Clarke R, et al. *In vitro* and *in vivo* antitumor properties of the cyclin dependent kinase inhibitor CYC202 (*R*-roscovitine). Int J Cancer 2002;102:463–8.

9. Fry DW, Harvey PJ, Keller PR, et al. Specific inhibition of cyclin-dependent kinase 4/6 by PD 0332991 and associated antitumor activity in human tumor xenografts. Mol Cancer Ther 2004;3:1427–38.

10. Misra RN, Xiao HY, Kim KS, et al. *N*-(cycloalkylamino)acyl-2-aminothiazole inhibitors of cyclin-dependent kinase 2. *N*-[5-[[[5-(1,1-dimethylethyl)-2-oxazolyl]methyl]thio]-2-thiazolyl]-4-piperidinecarboxamide (BMS-387032), a highly efficacious and selective antitumor agent. J Med Chem 2004;47:1719–28.

11. Garrett MD, Fattaey A. CDK inhibition and cancer therapy. Curr Opin Genet Dev 1999;9:104–11.

12. Chu XJ, DePinto W, Bartkovitz D, et al. Discovery of [4-amino-2-(1-methanesulfonylpiperidin-4-ylamino)pyrimidin-5-yl](2,3-diflu oro-6-methoxyphenyl)methanone (R547), a potent and selective cyclin-dependent kinase inhibitor with significant *in vivo* antitumor activity. J Med Chem 2006;49:6549–60.

13. DePinto W, Chu XJ, Yin X, et al. *In vitro* and *in vivo* activity of R547: a potent and selective cyclin-dependent kinase inhibitor currently in phase I clinical trials. Mol Cancer Ther 2006;5:2644–58.

14. Therasse P, Eisenhauer EA, Verweij J. RECIST revisited: a review of validation studies on tumour assessment. Eur J Cancer 2006;42: 1031–9.

15. Hilton H, Berkofsky-Fessler W, Kanwal C. The Data Cave: a collaborative method for interpreting genomic data. Eur Pharm Rev 2009;14:21–6.

16. Ensembl. 2008 Mar 2008 [cited 2008 Apr 22]; Ensembl release 49. Available from: http://www.ensembl.org/Homo_sapiens/geneview?gene=ENSG00000204537.

17. Freeman GJ, Gribben JG, Boussiotis VA, et al. Cloning of B7-2: a CTLA-4 counter-receptor that costimulates human T cell proliferation. Science 1993;262:909–11.

18. Shah R, Banks K, Patel A, et al. Intense expression of the b7-2 antigen presentation coactivator is an unfavorable prognostic indicator for differentiated thyroid carcinoma of children and adolescents. J Clin Endocrinol Metab 2002;87:4391–7.

19. Fahmy RG, Dass CR, Sun LQ, Chesterman CN, Khachigian LM. Transcription factor Egr-1 supports FGF-dependent angiogenesis during neovascularization and tumor growth. Nat Med 2003;9:1026–32.

20. Das A, Chendil D, Dey S, et al. Ionizing radiation down-regulates p53 protein in primary Egr-$1^{-/-}$ mouse embryonic fibroblast cells causing enhanced resistance to apoptosis. J Biol Chem 2001;276:3279–86.

21. Virolle T, Krones-Herzig A, Baron V, De Gregorio G, Adamson ED, Mercola D. Egr1 promotes growth and survival of prostate cancer cells. Identification of novel Egr1 target genes. J Biol Chem 2003; 278:11802–10.

22. Abdulkadir SA, Qu Z, Garabedian E, et al. Impaired prostate tumorigenesis in Egr1-deficient mice. Nat Med 2001;7:101–7.

23. Liu C, Rangnekar VM, Adamson E, Mercola D. Suppression of growth and transformation and induction of apoptosis by EGR-1. Cancer Gene Ther 1998;5:3–28.

24. Liu C, Adamson E, Mercola D. Transcription factor EGR-1 suppresses the growth and transformation of human HT-1080 fibrosarcoma cells by induction of transforming growth factor β1. Proc Natl Acad Sci U S A 1996;93:11831–6.

25. Huang RP, Fan Y, de Belle I, et al. Decreased Egr-1 expression in human, mouse and rat mammary cells and tissues correlates with tumor formation. Int J Cancer 1997;72:102–9.

26. Gerdes J, Lemke H, Baisch H, Wacker HH, Schwab U, Stein H. Cell cycle analysis of a cell proliferation-associated human nuclear antigen defined by the monoclonal antibody Ki-67. J Immunol 1984; 133:1710–5.

27. Mori Y, Sato F, Selaru FM, et al. Instabilotyping reveals unique mutational spectra in microsatellite-unstable gastric cancers. Cancer Res 2002; 62:3641–5.

28. Dudderidge TJ, Stoeber K, Loddo M, et al. Mcm2, Geminin, and KI67 define proliferative state and are prognostic markers in renal cell carcinoma. Clin Cancer Res 2005;11:2510–7.

29. Stearman RS, Dwyer-Nield L, Zerbe L, et al. Analysis of orthologous gene expression between human pulmonary adenocarcinoma and a carcinogen-induced murine model. Am J Pathol 2005;167:1763–75.

30. Zhu G, Reynolds L, Crnogorac-Jurcevic T, et al. Combination of

microdissection and microarray analysis to identify gene expression changes between differentially located tumour cells in breast cancer. Oncogene 2003;22:3742–8.

31. Pines J, Hunter T. Isolation of a human cyclin cDNA: evidence for cyclin mRNA and protein regulation in the cell cycle and for interaction with p34cdc2. Cell 1989;58:833–46.

32. Wierinckx A, Auger C, Devauchelle P, et al. A diagnostic marker set for invasion, proliferation, and aggressiveness of prolactin pituitary tumors. Endocr Relat Cancer 2007;14:887–900.

33. Chen Q, Zhang X, Jiang Q, Clarke PR, Zhang C. Cyclin B1 is localized to unattached kinetochores and contributes to efficient microtubule attachment and proper chromosome alignment during mitosis. Cell Res 2008;18:268–80.

34. Schmid MCD. Part III. Molecular and cellular hematology. Chapter 12. Cell cycle regulation and hematological disorders. In: Beutler ELM, Coller BS, Kipps TJ, Seligsohn U, editors. Williams hematology. 6th ed. McGraw-Hill; 2001, p. 131–40.

35. Eferl R, Ricci R, Kenner L, et al. Liver tumor development. c-Jun antagonizes the proapoptotic activity of p53. Cell 2003;112:181–92.

36. Kohoutek J, Blazek D, Peterlin BM. Hexim1 sequesters positive transcription elongation factor b from the class II transactivator on MHC class II promoters. Proc Natl Acad Sci U S A 2006;103:17349–54.

37. Peng J, Zhu Y, Milton JT, Price DH. Identification of multiple cyclin subunits of human P-TEFb. Genes Dev 1998;12:755–62.

38. Marshall NF, Peng J, Xie Z, Price DH. Control of RNA polymerase II elongation potential by a novel carboxyl-terminal domain kinase. J Biol Chem 1996;271:27176–83.

39. Yang Z, Yik JH, Chen R, et al. Recruitment of P-TEFb for stimulation of transcriptional elongation by the bromodomain protein Brd4. Mol Cell 2005;19:535–45.

40. Chandonia JM, Hon G, Walker NS, et al. The ASTRAL Compendium in 2004. Nucleic Acids Res 2004;32:D189–92.

41. Finn RD, Mistry J, Schuster-Bockler B, et al. Pfam: clans, web tools and services. Nucleic Acids Res 2006;34:D247–51.

42. Gress TM, Muller-Pillasch F, Geng M, et al. A pancreatic cancer-specific expression profile. Oncogene 1996;13:1819–30.

43. Fontemaggi G, Kela I, Amariglio N, et al. Identification of direct p73 target genes combining DNA microarray and chromatin immunoprecipitation analyses. J Biol Chem 2002;277:43359–68.

44. Agami R, Blandino G, Oren M, Shaul Y. Interaction of c-Abl and p73α and their collaboration to induce apoptosis. Nature 1999;399:809–13.

45. Foray N, Marot D, Gabriel A, et al. A subset of ATM- and ATR-dependent phosphorylation events requires the BRCA1 protein. EMBO J 2003;22:2860–71.